

SUPPLEMENTARY MATERIALS

TABLE SI
NMR structural statistics for the yeast Set2 SRI domain

	<SA> ¹	<SA> _{water-ref}
Number of NOE derived distance restraints		
All (unambiguous/ambiguous)	1958/198	
Long range i-j > 4 (unambiguous/ambiguous)	433/26	
R.m.s. deviation (Å) from experimental distance restraints ²		
R.m.s.d. (NOEs)	0.0147±0.0005	0.025±0.006
Hydrogen bonds (2*20)	0.026 ± 0.004	0.043 ± 0.006
R.m.s. deviation (°) from experimental torsion restraints ³		
R.m.s.d. (83 φ/ψ)	0.68 ± 0.07	0.88 ± 0.12
Coordinate Precision (Å) residues 10-94 ⁴		
N, C ⁻ , C [']	0.38 ± 0.06	0.48 ± 0.08
All heavy atoms	1.01 ± 0.05	1.05 ± 0.06
Structural quality ⁵		
Bad contacts	1.8 ± 0.8	0.0 ± 0.0
Ramachandran plot		
% in most favored region	90.2 ± 1.4	93.6 ± 1.6
% in additionally allowed region	9.4 ± 1.4	6.3 ± 1.6

¹<SA> is an ensemble of ten lowest-energy solution structures (out of 100 calculated) of the Set2 SRI domain before water-refinement. The CNS E_{repel} function was used to simulate van der Waals interactions with an energy constant of 25.0 kcal mol⁻¹ Å⁻⁴ using “PROLSQ” van der Waals radii; r.m.s. deviations for bond lengths, bond angles and improper dihedral angles are 0.0020 ± 0.0001 Å, 0.382 ± 0.008° and 0.31 ± 0.01°. 1 kcal = 4.18 kJ.

²Distance restraints were employed with a soft square-well potential using an energy constant of 50 kcal mol⁻¹ Å². For hydrogen bonds, distance restraints with bounds of 1.8-2.3 Å (H-O), and 2.8-3.3 Å (N-O) were derived for slow exchanging amide protons. No distance restraints were violated by more than 0.3 Å in the <SA> structures.

³Dihedral angle restraints derived from TALOS (27) were applied to backbone angles using energy constants of 200 kcal mol⁻¹ rad⁻². No dihedral angle restraint was violated by more than 5°.

⁴Coordinate precision is given as the Cartesian coordinate r.m.s. deviation of the 10 lowest-energy structures in the NMR ensemble with respect to their mean structure.

⁵Structural quality of the NMR ensemble was analyzed using PROCHECK (32).

FIG. S1 ^{15}N relaxation analysis of the Set2 SRI domain.

T_1 , T_2 and heteronuclear NOE data were measured at 292 K on a Bruker DRX 600 spectrometer as described (28). The correlation time for the rotational diffusion is $\tau_c \approx 9$ ns, consistent with a monomeric state of the SET2 SRI domain in solution. The T_1/T_2 ratio indicates regions of internal motion at time scales either above or below the overall tumbling correlation time, when the observed value differs significantly from the average T_1/T_2 ratio (upper panel). This suggests that residues 645-646 experience motion at slower time scales ($\tau > 9$ ns), while residue in the linkers connecting the helices are slightly more mobile on faster time scales ($\tau < 9$ ns). Heteronuclear $\{^1\text{H}\}$ - ^{15}N NOE values below 0.6 represent backbone amides of residues that undergo fast internal motion (lower panel), and are only observed for N- and C-terminal residues.

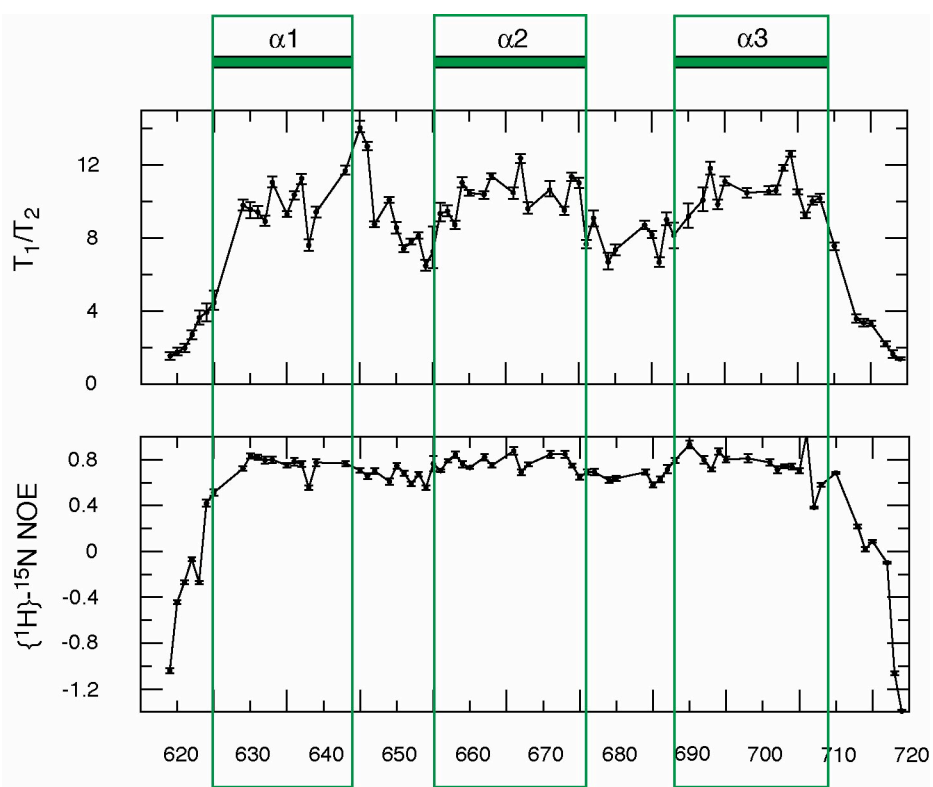


FIG. S2. Comparison of the Set2 SRI domain with known helical CTD-binding folds.

The structures are shown as ribbon models colored from blue to red from the N- to the C-terminus, respectively. Shown are from left to right: the Set2 SRI domain (this study), an FF domain (33), and the Pcf11 CID domain (34). For orientation of the structures, the N-terminal helices were superimposed. Note that the SRI domain shows a left-handed superhelical arrangement, whereas the two other domains adopt a right-handed arrangement.

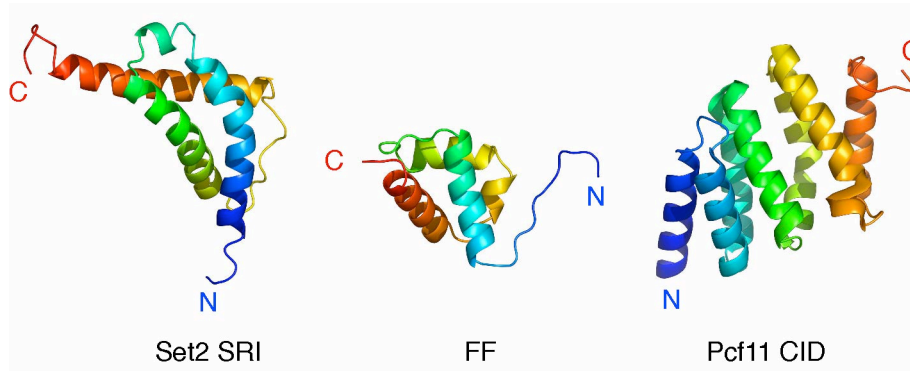


FIG. S3. NMR-monitored CTD binding of the Set2 SRI domain.

(A) Sequence of the two CTD peptides used for binding studies. The upper peptide did not bind the SRI domain, the lower peptide bound with an apparent dissociation constant in the low μM range. (B) NMR titration experiment. Shown are 2D ^1H , ^{15}N -HSQC spectra before (black) and after (red) addition of a 1.25-molar excess of the two-repeat peptide shown in (A). Residues that show strong chemical shift perturbations are labeled.

